Agilent

Trusted Answers

Research Citation Collection

Selected publications featuring Agilent Automated Electrophoresis instruments for infectious disease research

Objective Sample Quality Control for Infectious Disease Research

Infectious diseases are caused by many different organisms including bacteria, viruses, fungi, and parasites that penetrate the body's natural barriers, causing a range of symptoms from non-detectable to deadly. Transmission is as varied as the organisms themselves. Some infectious diseases are passed from person to person, others by insects or animals. Some, such as bacteria and parasites are transmitted via consumption of contaminated food or water. Occasionally, infectious diseases can become a worldwide threat because of resistance to antibiotics and treatments or emergence of a novel variant, necessitating global surveillance and response. Outbreaks, especially among farmed animals and in fisheries, can lead to widespread mortality and devastating economic loss for businesses. Continued research on microbial diseases is necessary for prevention, detection, controlling spread, and treatment.

Automated electrophoresis is a powerful tool for microbial, fungal, and viral nucleic acid analysis. The Agilent Fragment Analyzer, Agilent TapeStation, and Agilent Bioanalyzer systems provide a fast and effective method for sample quality control as part of the workflow for genomic analysis applications such as next generation sequencing (NGS) or new method development. In addition, they deliver reliable sizing for a variety of fragment analysis applications that directly identify biomarkers of interest. The Bioanalyzer, Fragment Analyzer, and TapeStation are the foremost utilized instruments for RNA analysis.

In this compendium, we've provided synopses of nine peer-reviewed publications to illustrate the numerous ways the Agilent automated electrophoresis systems were utilized for the analysis of different infectious diseases. The electrophoresis instruments analyzed RNA and DNA in order to detect an amplicon size difference for a new gene variant, prokaryotic RNA, teasing out activated cell host pathways through RNA degradation, detection of bacteria through enzyme digestion patterns, new assay development, and bacterial cleavage of RNA. See how researchers learned more about SARS-CoV-2, *human papillomaviruses*, *Pseudomonas aeruginosa*, *Piscirickettsia salmonis*, *Ostreid herpesvirus 1*, *Shuni virus*, *Mardivirus*, and *Chlamydophila abortus* with the Agilent electrophoresis instruments.

Table of Contents

A Deletion in SARS-CoV-2 ORF7 Identified in COVID-19 Outbreak in Uruguay

Transbound. Emerg. Dis., **2021**, 10, 1-8

Authors

Y. Panzera, N. Ramos, S. Frabasile, L. Calleros, A. Marandino, G. Tomás, C. Techera, S. Grecco, E. Fuques, N. Goñi, V. Ramas, L. Coppola, H. Chiparelli, C. Sorhouet, C. Mogdasy, J. Arbiza, A. Delfraro, and R. Pérez

Synopsis

The genetic diversity of the SARS-CoV-2 virus has been followed carefully in order to provide insights into how the virus emerged and continues to evolve. Tracking the genetic evolution of the virus allows scientists to identify more virulent or deadly strains. The most common genetic variations to date in SARS CoV-2 are single or point mutations. Indels have also been identified, albeit less frequently, and provide information about the robustness of the virus' functionality. Scientists in Uruguay analyzed an outbreak of 14 patients and detected a 12-nucleotide deletion in the ORF7a accessory gene. Quality control and length of the sequencing libraries were assessed on the 5200 Fragment Analyzer. In addition, the deletion was confirmed with the Fragment Analyzer and the Agilent High Sensitivity NGS kit by detecting a size difference between the deleted and wild-type amplicons (Figure 1) followed by Sanger sequencing.

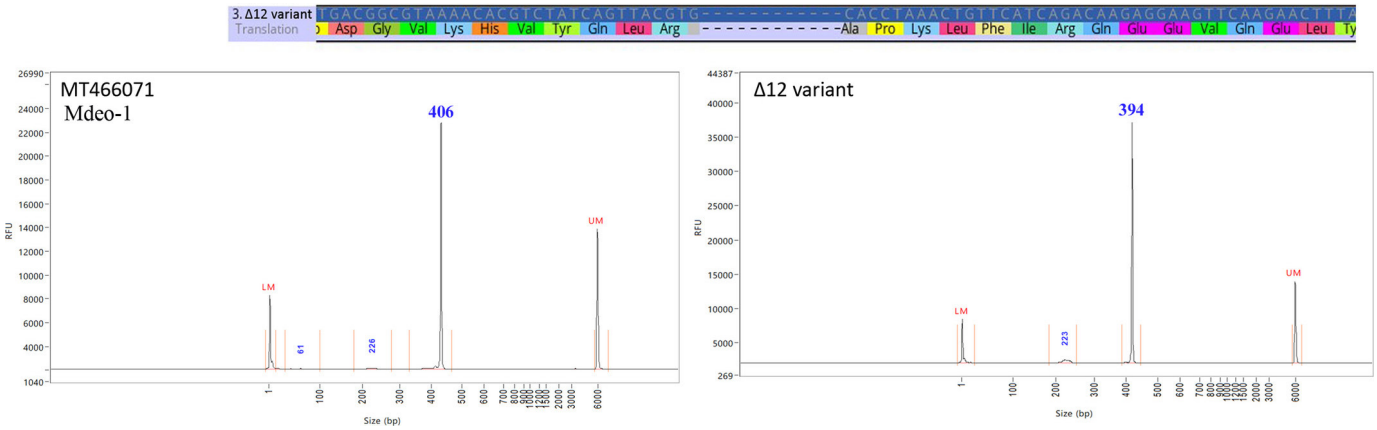

Figure 1. Amplicon capillary electrophoresis analysis. Chromatogram peaks using Mdeo-1 reference sequence (MT466071) and Δ12 variant, left and right, respectively. This figure was excerpted from Panzera *et al*.

Early Endonuclease-Mediated Evasion of RNA Sensing Ensures Efficient Coronavirus Replication

PLOS Pathog., **2017**; 13(2):e1006195

Authors

E. Kindler, C. Gil-Cruz, J. Spanier, Y. Li, J. Wilhelm, H.H. Rabouw, R. Züst, M. Hwang, P. V'kovski, H. Stalder, S. Marti, M. Habjan, L. Cervantes-Barragan, R. Elliot, N. Karl, C. Gaughan, F.J.M. van Kuppeveld, R.H. Silverman, M. Keller, B. Ludewig, C.C. Bergmann, J. Ziebuhr, S.R. Weiss, U. Kalinke, and V. Thiel

Synopsis

Coronaviruses are known to efficiently evade early innate immune responses that restrict virus replication and spread. The highly conserved coronavirus endonucleolytic activity (EndoU) on single-stranded and double-stranded RNA is found in viruses that evade many vertebrate hosts. It is co-expressed with other key replicative proteins but is not essential for viral RNA synthesis. EndoU-deficient mutants of human coronavirus 229E (HCoV-229E) and mouse hepatitis virus (MHV) were assessed for replication titers and activated host pathways. The Fragment Analyzer system with the Agilent Standard Sensitivity RNA kit (15 nt) assessed the integrity of RNA and identified degradation of ribosomal RNA (Figure 5) as a marker for host pathway involvement. By monitoring host dsRNA response with the Fragment Analyzer, it was determined that the coronavirus EndoU activity is key to preventing early induction of multiple host cell dsRNA sensors that are responsible for sensing viral infection.

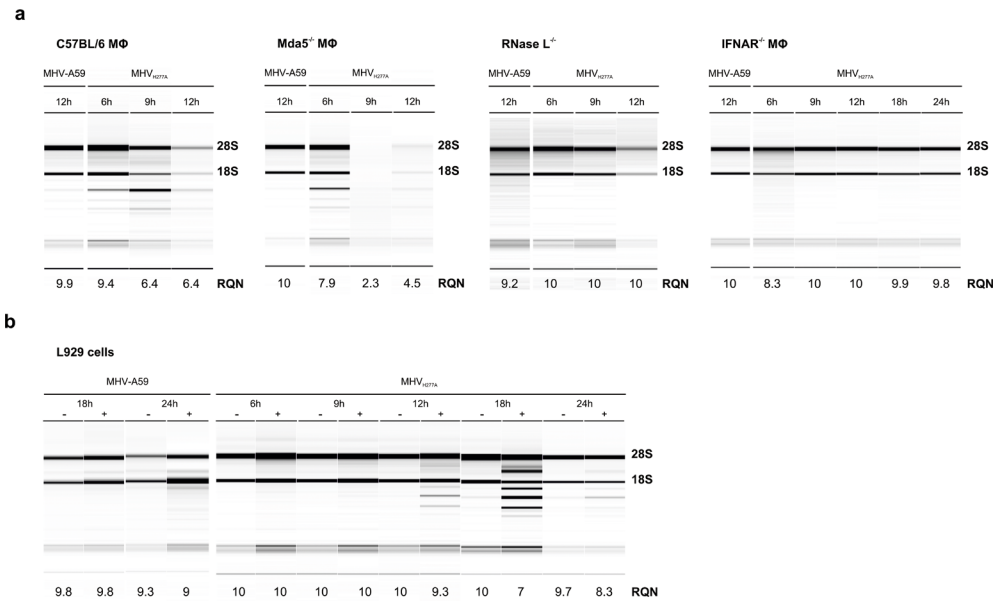

Figure 5. EndoU-deficient MHV induces activation of the OAS-RNase L pathway, resulting in early breakdown of ribosomal RNA. (a) Analysis of rRNA integrity in bone marrow-derived macrophages derived from wild type C57BL/6, Mda5$^{-/-}$, RNase L$^{-/-}$, and IFNAR$^{-/-}$ mice following infection with MHV-A59 and MHV$_{H277A}$ (MOI=1). Total RNA was isolated at indicated time points and degradation of ribosomal RNA as marker for RNase L activation was assessed with a Fragment Analyzer. One representative picture and migration of 18S and 28S ribosomal RNA is displayed. The RNA Quality Number (RQN) is indicated. (b) The integrity of rRNA from MHV-A59 and MHV$_{H277A}$ infected (MOI=1) L929 cells, with or without IFN-I pre-treatment (12.5 U of IFN-I 16 h prior to infection). Analysis was performed as in panel (a) and one representative image out of five is displayed. This figure has been reproduced from Kindler *et al*.

HPV Insertional Pattern as a Personalized Tumor Marker for the Optimized Tumor Diagnosis and Follow-up of Patients with HPV-Associated Carcinomas: A Case Report

BMC Cancer **2019**, 19(277)

Authors

Alexandre Harlé, Julie Guillet, Jacques Thomas, Jessica Demange, Gilles Dolivet, Didier Peiffert, Agnès Leroux, and Xavier Sastre-Garau

Synopsis

Specific genotypes of human papillomaviruses (HPV) are associated with numerous carcinomas in the anogenital, head, and neck regions. The presence of HPV has been suggested as a prognostic indicator for cervical, head, and neck cancers. The lack of development of HPV markers has limited the molecular characterization of HPV DNA sequences. The capture-based next-generation sequencing (NGS) (CaptHPV) assay was designed to provide a comprehensive molecular characterization of HPV DNA sequences including identification of the physical state, viral load, insertion site, and presence of genomic alterations in the specimen for 245 different HPV genotypes. For research purposes, CaptHPV analysis was performed on two tumors of the tongue and anal canal with primers specific for HPV16, HPV18, and consensus GP5/GP6 primers. Subsequent fragment analysis with the Fragment Analyzer system detected HPV16 DNA sequence in both tumor specimens (Figure 3). Further analysis with CaptHPV identified the same HPV16 DNA sequences and integration pattern in the two tumors. CaptHPV analysis of HPV sequences and integration patterns can aid in determining tumor independence or metastasis.

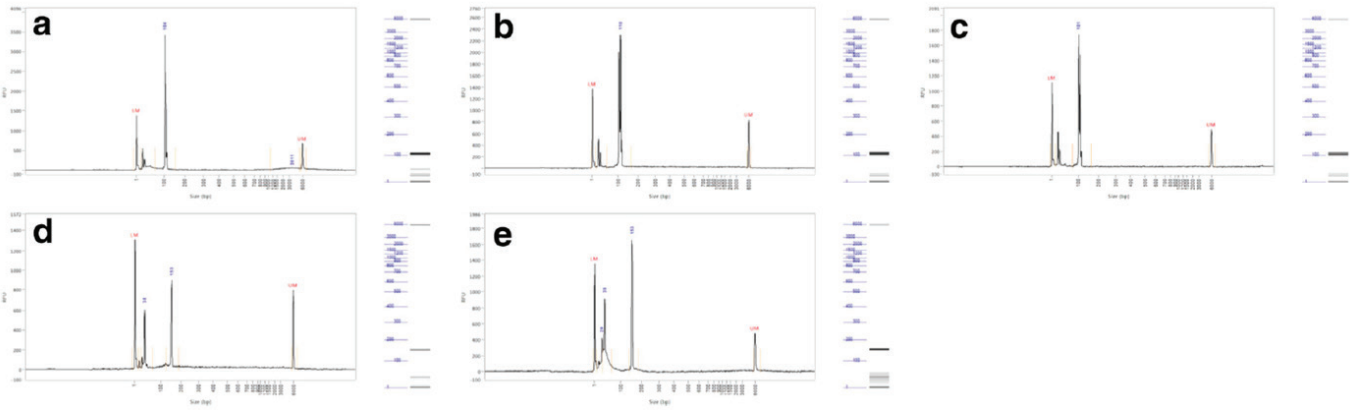

Figure 3. PCR migration profiles using Fragment Analyzer. HPV16 amplification have been found in both lingual tumor and anal carcinoma with relative fluorescence unit (RFU) of 3411, 2298, and 1740 for lingual tumor (a), anal carcinoma (b), and positive control (c) respectively and amplification of HPV consensus has only been found in anal carcinoma relative fluorescence with RFU of 901 and 1654 for anal carcinoma (d) and positive control (e) respectively. LM: Lower Marker; UM: Upper Marker. This figure has been reproduced from Harlé *et al*.

Pseudomonas aeruginosa Cleaves the Decoding Center of *Caenorhabditis elegans* Ribosomes

PLOS Biol., **2020**, 18(12): e3000969

Authors

Alejandro Vasquez-Rifo, Emiliano P. Ricci, and Victor Ambros

Synopsis

Pseudomonas aeruginosa is a proteobacteria that infects a wide range of animal hosts including humans. The interaction between *Caenorhabditis elegans* and *P. aeruginosa* strain PA14 is a well studied, model host-pathogen interaction. One way the bacteria exploits the *C. elegans* host is by inhibiting translation through the exotoxin A protein, but multiple pathways could be involved. The 5300 Fragment Analyzer system and Standard Sensitivity RNA kit (15 nt) were used to investigate the effects of the *P. aeruginosa* strain PA14 on the ribosomes of *C. elegans*. The Fragment Analyzer electropherogram showed that after exposure to *P. aeruginosa* PA14, *C. elegans* total RNA displayed two additional peaks at 1,100 and 2,300 nt that were not observed in worms fed *E. coli* HB101 (Figure 1A). Through sequencing, these peaks were identified as fragments of the 26S rRNA, cleaved in the highly conserved H69 loop. The Fragment Analyzer was also used to monitor the accumulation of the two 26S fragments relative to the total 26S rRNA pool. After 24 hours of exposure, an average of 25% of the worm 26S rRNA consisted of cleaved fragments. In addition, the Fragment Analyzer was used to determine if stress conditions or other bacteria induced cleavage of the 26S rRNA in *C. elegans*. No other stressors or bacteria induced rRNA cleavage (see paper Figure S1A).

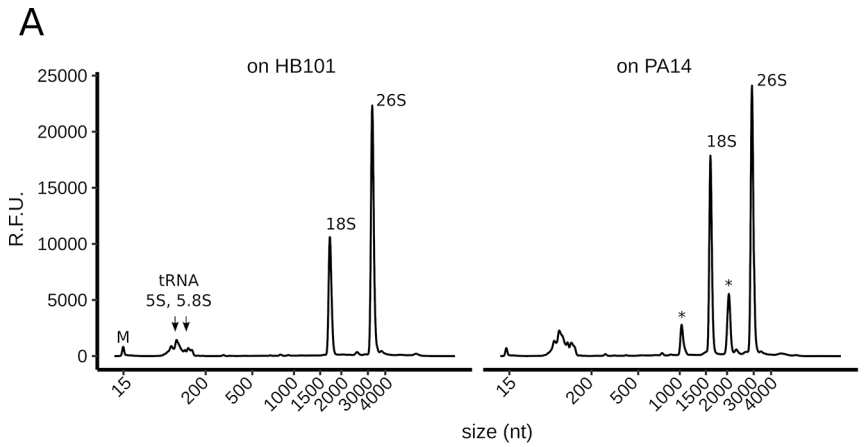

Figure 1. Effects of *P. aeruginosa* PA14 on the rRNA of *C.elegans* worms. (A) Total RNA profile of adult worms exposed for 24 h to *P. ae*. PA14 (right panel) or *Escherichia coli* HB101 (left panel). Asterics indicate the 2 most abundant bands that appear upon PA14 exposure. "M" indicates a 15-nt marker used in the electrophoretic separation system. This figure was excerpted from Vasquez-Rifo *et al*.

A Single-Tube HNB-Based Loop-Mediated Isothermal Amplification for the Robust Detection of the *Ostreid herpesvirus* 1

Int. J. MOL. Sci., **2020**, 21(18), 6605

Authors

Maja A. Zaczek-Moczydłowska, Letitia Mohamed-Smith, Anna Toldrá, Chantelle Hooper, Mònica Campàs, M. Dolors Furones, Tim P. Bean, and Katrina Campbell

Synopsis

The *Ostreid herpesvirus* 1 (OsHV-1) has been identified globally as the cause of significant disease outbreaks and losses in shellfish farming. A simple onsite screening method with rapid reaction times and simple equipment requirements is needed for early detection and prevention of the onset and spread of disease. A simple colorimetric loop-mediated isothermal amplification (LAMP) assay with hydroxynaphthol blue (HNB) was developed for the detection of OsHV-1 and its variants infecting *Crassostrea gigas*. The optimized assay for the LAMP primers displayed an amplified product on the TapeStation system ranging from 90 to 1,000 bp, while no amplification peak was detected for the negative control (NTC). The colorimetric detection correlated with the TapeStation, violet for negative control, and blue for OsHV-1 amplification product. The TapeStation system was utilized at every step of assay development "*for its efficiency to analyze LAMP products for the optimal concentration of reagents, primer-dimer formation and artifacts that are not easily detected or possibly visualized on gel by standard electrophoresis-based methods*".

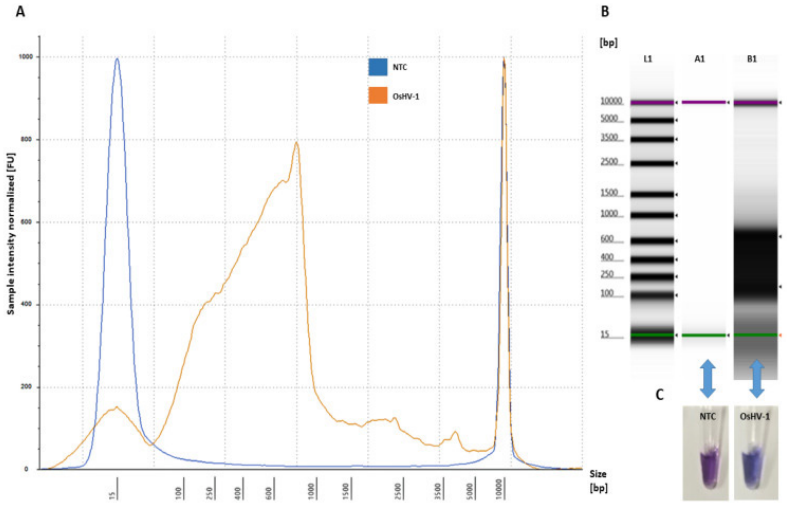

Figure 3. Amplification of OsHV-1 by LAMP assay: (A) electropherogram profile comparison of NTC (blue) and positive sample (OsHV-1 DNA-plasmid) (orange) analyzed using TapeStation Analysis software A.02.02 with a progressive increase of the amplified LAMP product showing a size shift of 90 – 1,000 bp; (B) gel image profile comparison: (L1) – ladder 15 – 5,000 bp, (A1) – NTC and (B1) – positive samples showing a single high molecular band smear-like pattern (90 – 1,000 bp) of the amplified LAMP product visualized using TapeStation Analysis software A.02.02; and (C) NC (violet) and positive samples (OsHV-1 DNA-plasmid) (blue) visualized using HNB. This figure has been reproduced from Zaczek-Moczydłowska *et al*.

Reverse Genetics System for Shuni Virus, an Emerging *Orthobunyavirus* with Zoonotic Potential

Viruses, **2020**, 12(4), 455

Authors

Judith Oymans, Paul J. Wichgers Schreur, Sophie van Oort, Rianka Vloet, Marietjie Venter, Gorben P. Pijlman, Monique M. van Oers, and Jeroen Kortekaas

Synopsis

The genus *Orthobunyavirus* comprises 170 different mosquito- and midge-borne viruses, several of which cause severe disease in animals and humans. Their three-segmented genomes (L, M, and S) enable reassortment with related viruses, creating the potential for a novel virus as seen with the Schmallenberg virus (SBV) affecting cows in north-western Europe in 2011. The Shuni virus (SHUV) is related to the Schmallenberg virus and has been found to infect cows, horses, sheep, and goats through both midges and mosquitoes. Researchers developed a reverse genetics system for SHUV to evaluate the viability of reassortants between SBV and SHUV. To confirm the identity of the recombinant wild type and reassortant viruses, PCR was performed with varied primers and analyzed with the TapeStation system and Agilent D1000 ScreenTape assay (Figure 2). Visualization with the TapeStation system confirmed a successful rescue of a virus containing the segments from SBV-L and -S and SHUV-M, suggesting that such a reassortant could emerge in the field.

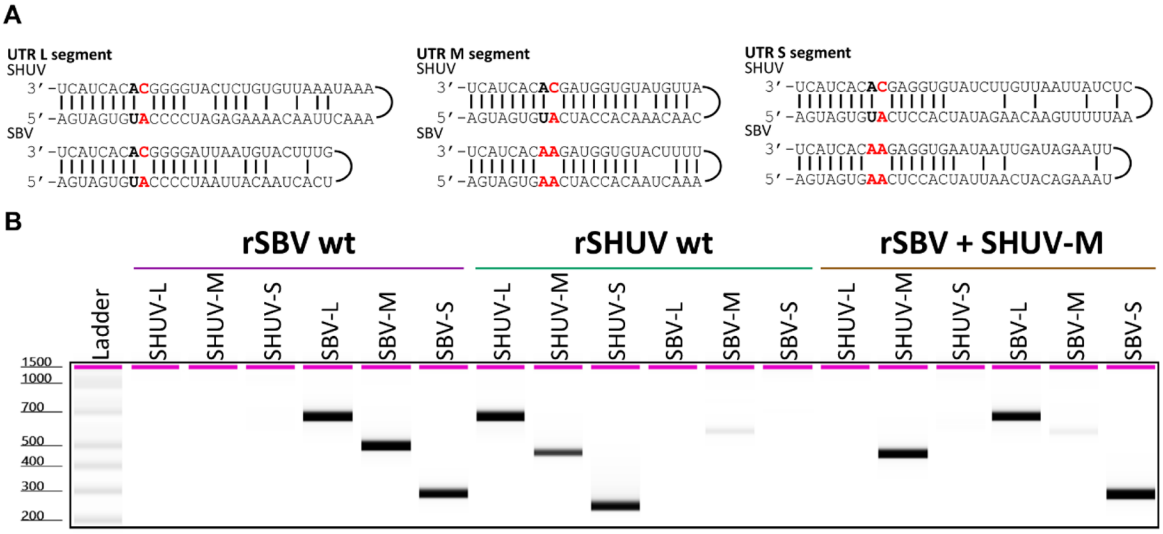

Figure 2. Characterization of a Schmallenberg virus (SBV) – (SHUV) reassortant. (A) The alignment of the UTRs of SBV and SHUV. SHUV contains a single mismatch at position 9, while SBV contains a double mismatch at positions 8 and 9 (indicated in red) in the UTR of the M and S segment. (B) The identity of the reassortant was confirmed by PCR using primers specifically recognizing SBV or SHUV L-, M-, or S-segments. PCR products were analyzed with the TapeStation system. This figure has been reproduced from Oymans *et al*.

 Oymans J, Wichgers Schreur PJ, van Oort S, et al. Reverse Genetics System for Shuni Virus, an Emerging Orthobunyavirus with Zoonotic Potential. *Viruses*. **2020**;12(4):455. Published 2020 Apr 17. doi:10.3390/v12040455

Comparison of the Transcriptomes and Proteomes of Serum Exosomes from Marek's Disease Virus-Vaccinated and Protected and Lymphoma-Bearing Chickens

Genes (Basel) **2019**, 10(2), 116

Authors

Sabari Nath Neerukonda, Phaedra Tavlarides-Hontz, Fiona McCarthy, Kenneth Pendarvis, and Mark S. Parcells

Synopsis

Marek's disease of chickens is caused by Marek's disease virus (MDV) and manifests in complex pathology including paralysis, immunosuppression, and T-cell lymphomagenesis. Marek's disease is controlled by vaccination *in ovo* or at hatch, which protects chicken against lymphoma formation but not against superinfection by MDV field strains. Vaccine induces humoral and cell-mediated immunity. However, mechanisms eliciting systemic protection are unclear. The study demonstrates the role of serum exosomes as indicators of systemic immunity and tumor formation. RNA isolated from exosomes were analyzed using the Bioanalyzer system, demonstrating the presence of RNA with the expected yields, size distribution, and profiles of typical exosomal samples (Figure 2). In addition, the Bioanalyzer confirmed the absence of ribosomal RNA. Subsequent small RNA sequencing analysis revealed distinguishing gene expression signatures between vaccinated and tumor-bearing chickens.

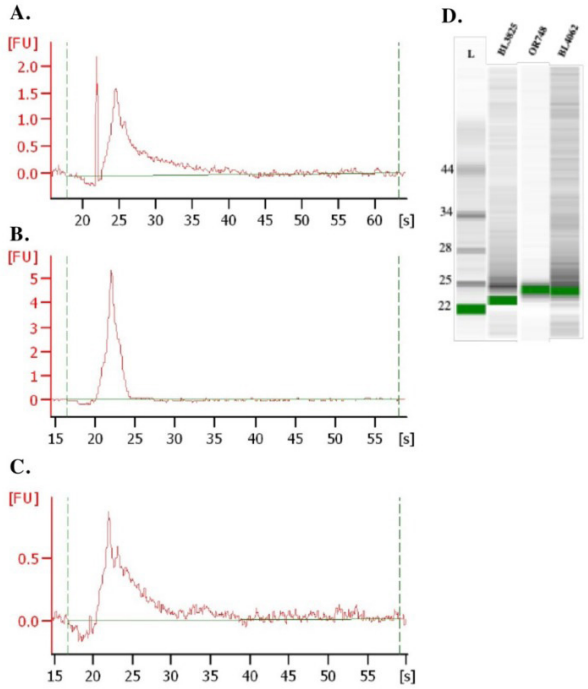

Figure 2. Size distribution of exosomal RNAs. Panels (A–C) show fluorograms of exosomal RNAs determined by the Agilent RNA Pico Chip. Panel (A) shows fluorogram of exosomal RNA from vaccinated leghorn chickens (VEX), unvaccinated tumor-bearing leghorn chickens (TEX) (B), and broiler chickens TEX (C). Panel (D) shows RNA chip analyses of purified exosomal RNAs. This figure has been reproduced from Neerukonda *et al.*

 Neerukonda SN, Tavlarides-Hontz P, McCarthy F, Pendarvis K, Parcells MS. Comparison of the Transcriptomes and Proteomes of Serum Exosomes from Marek's Disease Virus-Vaccinated and Protected and Lymphoma-Bearing Chickens. *Genes (Basel)*. **2019**;10(2):116. Published 2019 Feb 5. doi:10.3390/genes10020116

Transcriptional Analysis of in vitro Expression Patterns of *Chlamydophila abortus* Polymorphic Outer Membrane Proteins During the Chlamydial Developmental Cycle

Vet. Res. **2009**, 40(5), 47

Authors

Nicholas Wheelhouse, Kevin Aitchison, Lucy Spalding, Morag Livingstone, and David Longbottom

Synopsis

The most common cause of bovine enzootic abortion is *Chlamydophila abortus*. It is also a common cause of lamb mortality in most sheep-rearing areas in the world. Polymorphic membrane proteins (Pmps) of *C. abortus* play an important role in chlamydial pathogenesis. In this study, McCoy cells were infected with *C. abortus* followed by total RNA isolation and gene expression analysis at different time-points. The Bioanalyzer system was employed to detect the host eukaryotic RNA and the *C. abortus* prokaryotic RNA expression (Figure 1). Eukaryotic RNA has a typical RNA profile with two main peaks, 18S and 28S rRNA. After 48 hours of infection with *C. abortus*, RNA extracted from the host cells displayed a profile with four rRNA peaks, representing a mixture of eukaryotic and prokaryotic rRNA. Differential expression patterns of mRNAs coding for different Pmps during the developmental cycle of *C. abortus* suggest a role of some Pmps in antigenic variation during chlamydial pathogenesis.

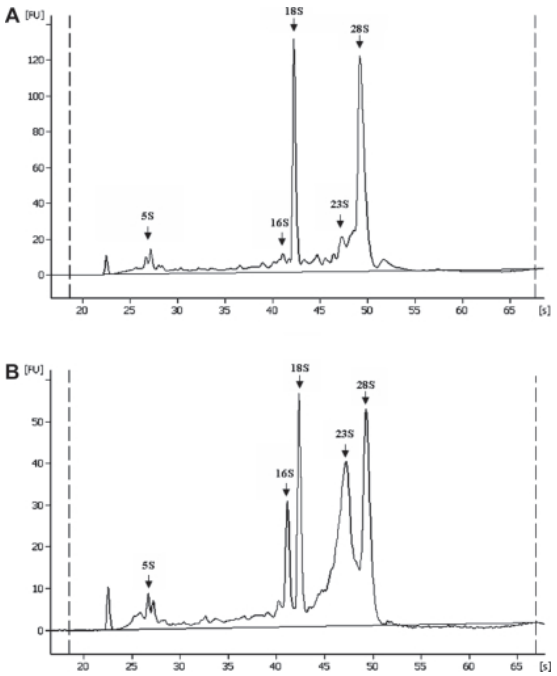

Figure 1. Electropherograms of total RNA isolated from *C. abortus*-infected McCoy cells at two time points in the chlamydial developmental cycle. The presence of both eukaryotic (28S, 18S, 5S) and prokaryotic (chlamydial) (23S, 16S, 5S) RNA is indicated at 24 h p.i. (A) and 48 h p.i. (B). This figure has been reproduced from Wheelhouse *et al*.

 Wheelhouse N, Aitchison K, Spalding L, Livingstone M, Longbottom D. Transcriptional analysis of in vitro expression patterns of *Chlamydophila abortus* polymorphic outer membrane proteins during the chlamydial developmental cycle. *Vet Res*. **2009**;40(5):47. doi:10.1051/vetres/2009030

Genomic-Based Restriction Enzyme Selection for Specific Detection of *Piscirickettsia salmonis* by 16S rDNA PCR-RLP

Front. Microbiol., **2016**, 7, 643

Authors

Dinka Mandakovic, Benjamín Glasner, Jonathan Maldonado, Pamela Aravena, Mauricio González, Verónica Cambiazo, and Rodrigo Pulgar

Synopsis

Piscirickettsia salmonis is a gram-negative bacterium that can infect, replicate, and propagate in several fish lines causing salmonid rickettsial septocaemia (SRS). Outbreaks occur across the globe despite vaccine and antibiotic treatments, causing great economic losses for the global salmon farming industry. A better diagnostic method was needed to detect *P. salmonis* with greater sensitivity and distinguish it from other bacteria that coexist and contaminate samples. Restriction enzymes were identified that generated a unique *P. salmonis* 16S rDNA (recombinant DNA) band pattern to be used in a new PCR-RFLP assay. The TapeStation system was used to determine if the *PmaCI* band pattern of *P. salmonis* 16S rDNA could be distinguished from 11 other bacteria that are commonly co-infected or contaminated in the samples. The TapeStation results (Figure 2C) were compared to expected digest band patterns (Figure 2A) and gel electrophoresis (Figure 2B), with both methods demonstrating the same distinct *Pma*CI digest band pattern for *P. salmonis*. In addition, the detection limit of the *PmaCI* PCR-RFLP assay was evaluated with the TapeStation system (see paper Supplementary Figure 3). The TapeStation had a lower limit of detection (0.25 ng) compared to agarose gel (250 ng). The authors pointed out that "*visualization is widely improved (0.25 ng, 1000-fold improved) using the ScreenTape technology with the 2200 TapeStation system…Moreover, the High Sensitivity D5000 ScreenTape assay promises to further improve this detection limit to 0.01 ng, which will give remarkable sensibility to all PCR based methods*". It was also determined, through visualization with the TapeStation software, that the same digestion pattern for *P. salmonis* was detectable when co-infected with different proportions of *V. anguillarum* (see paper Figure 4). This restriction digest method provided a more specific, faster, and cheaper assay than the *P. salmonis* detection methods currently available.

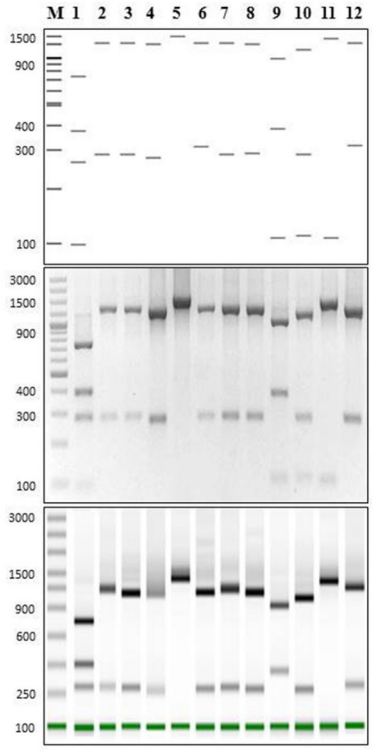

Figure 2. PCR-RFLP for *P. salmonis* and cohabitant strains using *PmaCI* restriction enzyme. (Upper panel) Predicted digestion patterns of 16S rDNA using NEBcutter web tool for all bacterial strains used in this study. (Middle panel) 2% gel electrophoresis showing PCR-RFLP digestion pattern (16SrDNA amplification using primers 27F/1492R) for all bacterial strains used in this study. (Lower pane) TapeStation 2200 screening of PCR-RFLP digestion pattern of samples in B. In all cases: 1, *Piscirickettsia salmonis* LF-89; 2, *Vibrio anguillarum* INTA11; 3, *Aeromonas salmonicida* INTA1; 4, *Flavobacterium psychrophilum* INTA9; 5 *Renibacterium salmoninarum* INTA10; 6, *Shewanella frigidimarina* INTA2; 7, *Photobacterium phosphoreum* INTA3; 8, *Psychrobacter nivimaris* INTA4; 9, *Arthrobacter oxydans* INTA5; 10, *Staphylococcus saprophyricus* INTA6; 11, *Microbacterium lacus* INTA7; 12, *Escherichia coli* INTA8. M, O'GeneRuler 100 bp DNA Ladder Plus (bp). This figure has been reproduced from Mandakovic *et al.*

Learn more:

www.agilent.com/genomics/automated-electrophoresis
www.agilent.com/en/solutions/infectious-disease

Buy online:

www.agilent.com/chem/store

U.S. and Canada
1-800-227-9770
agilent_inquireies@agilent.com

Europe
info_agilent@agilent.com

Asia Pacific
inquiry_lsca@agilent.com

PR7000-8146

Published in the USA, August 20, 2021
5994-3942EN

Agilent
Trusted Answers